

Supplement of Atmos. Chem. Phys., 20, 9871–9882, 2020
<https://doi.org/10.5194/acp-20-9871-2020-supplement>
© Author(s) 2020. This work is distributed under
the Creative Commons Attribution 4.0 License.



Supplement of

Tracking separate contributions of diesel and gasoline vehicles to roadside PM_{2.5} through online monitoring of volatile organic compounds and PM_{2.5} organic and elemental carbon: a 6-year study in Hong Kong

Yee Ka Wong et al.

Correspondence to: Jian Zhen Yu (jian.yu@ust.hk)

The copyright of individual parts of the supplement might differ from the CC BY 4.0 License.

S1. Sampling and quality control work for hourly OC–EC measurement

Ambient air was drawn through a 2.5 μm aerodynamic diameter cut-point cyclone and a parallel-plate carbon filter organic denuder (Sunset Laboratory, OR, USA) at a designated flow rate of 8.0 L min^{-1} (local condition) for the first 46 min of the hourly cycle to collect $\text{PM}_{2.5}$ samples. The PM deposited on a pre-baked quartz filter substrate then underwent a 9 min OC–EC analysis with a thermal-optical method following the modified National Institute for Occupational Safety and Health (NIOSH) method 5040 protocol (Turpin et al., 1990; Birch and Cary, 1996; NIOSH, 2003). In particular, the carbon evolved before the laser transmittance signal returns to the initial value is counted as OC, while that evolved after the split point is classified as EC. Finally, the instrument was stabilized for 3 min before the sampling of the next cycle begins.

A list of on-site quality control work was performed during instrument operation to ensure adequate sample collection and analysis, as shown Table S1. Results for recovery of sucrose external calibration check, instrument blank, method detection limit (MDL) and dynamic blank test (i.e., OC associated with organic vapor adsorption) by calendar year are summarized in Table S2. The MDL in $\mu\text{g C m}^{-3}$ was calculated as 3 times the standard deviation of the instrument blank values divided by the volume of air sampled in one analysis (i.e., $0.008 \text{ m}^3 \text{ min}^{-1} \times 46 \text{ min}$).

The collected data were processed by the Sunset Laboratory OC/EC Analysis Program. Level I data validation was performed through checking the sampling volume, calibration peak area, laser signal and non-dispersive infra-red (NDIR) response.

S2. PMF modeling details

Species input uncertainties: For concentrations above the MDL, the input uncertainties for $\text{PM}_{2.5}$ OC and EC were propagated from the instrument analytical uncertainty and sampling flow uncertainty (5 %). The input uncertainties for VOCs, NO_x and CO were calculated by Eq. (S1) according to the EPA PMF User Guide (Norris et al., 2014):

$$\text{Uncertainty} = \sqrt{(\text{Error fraction} \times \text{Concentration})^2 + (0.5 \times \text{MDL})^2} \quad (\text{S1})$$

where the error fraction is assumed to be 0.2 for these species (except ethane and ethene where 0.4 was adopted because of peak overlapping issue in GC separation), MDLs for VOCs were determined by HKEPD on a monthly basis and MDLs for NO_x and CO were adopted from the instrument specification. It is reported the precisions of VOC measurement using the same instrument at MK AQMS range between 2.5–20 % depending on species identity (Lyu et al., 2016). For all species, concentrations below the MDL were replaced by $0.5 \times \text{MDL}$ with $5/6 \times \text{MDL}$ being the uncertainty.

S3. PMF uncertainty analysis results

Displacement (DISP): DISP analysis was performed on the base (considering all samples) and grouped (samples divided into three groups of same size) PMF solutions. In DISP analysis, the species of all resolved profiles are perturbed to investigate the largest range of factor profile values without violating a range of designated Q values. It explores the rotational ambiguity of the solutions. For all solutions (base and grouped), the maximum change in Q value $dQ = 0$, indicating the Q values of the solutions have reached the global minimum. More importantly, no factor swap was noted, indicating the solutions obtained are rotationally robust. The uncertainties related to source contributions are less than those derived from the bootstrap analyses and therefore are not reported here.

Fpeak: Fpeak analysis was also performed on the base PMF solution using Fpeak values (strengths) of -5 and 5 . The resulting % dQ is 0.02 – 0.03 %, indicating the solution is robust in a rotational sense. Also, the Fpeak execution exerted negligible influence on the source contribution and profile matrices resolved.

Bootstrap (BS): BS was performed on the grouped samples to evaluate the potential effect of a small fraction of samples on the solutions, i.e., the random error of the solutions. In each execution, 100 BS runs were performed. For all BS analyses, all BS factors could map with the base factors. The BS results in terms of uncertainties associated with source contributions to OC_{vehicle} , EC_{vehicle} and PM_{vehicle} are illustrated as shaded area in Fig. S11a–c. These areas are constructed using the monthly average of the 5th and 95th percentile of the BS solutions.

References

- Birch, M. E. and Cary, R. A.: Elemental carbon-based method for monitoring occupational exposures to particulate diesel exhaust, *Aerosol Sci. Technol.*, 25, 221–241, 1996.
- Lyu, X. P., Guo, H., Simpson, I. J., Meinardi, S., Louie, P. K. K., Ling, Z. H., Wang, Y., Liu, M., Luk, C. W. Y., Wang, N., and Blake, D. R.: Effectiveness of replacing catalytic converters in LPG-fueled vehicles in Hong Kong, *Atmos. Chem. Phys.*, 16, 6609–6626, 2016.
- NIOSH: Monitoring of diesel particulate exhaust in the workplace, Third supplement to Manual of Analytical Methods, 4th Edition, Cincinnati, OH, Publication No. 2003–154, 2003.
- Norris, G., Duvall, R., Brown, S., and Bai, S.: EPA Positive Matrix Factorization (PMF) 5.0 Fundamentals and User Guide, U.S. Environmental Protection Agency, Washington, DC, 2014.
- Tsai, W. Y., Chan, L. Y., Blake, D. R., and Chu, K. W.: Vehicular fuel composition and atmospheric emissions in south China: Hong Kong, Macau, Guangzhou, and Zhuhai, *Atmos. Chem. Phys.*, 6, 3281–3288, 2006.
- Turpin, B. J., Cary, R. A., and Huntzicker, J. J.: An in-situ, time-resolved analyzer for aerosol organic and elemental carbon, *Aerosol Sci. Technol.*, 12, 161–171, 1990.

Table S1. Quality control work for semi-continuous OC–EC field analyzer operation in this study

Quality control work	Frequency
<ul style="list-style-type: none">• On-site check of the analyzer condition for any error flags that show hardware problems	1–2 times every week
<ul style="list-style-type: none">• Filter replacement• Single-point sucrose external calibration check using 5 μL of 4.27 $\mu\text{g C } \mu\text{L}^{-1}$ sucrose standard (see Table S2 for results)• Instrument blank (see Table S2 for results)• Auto-zero of the carrier gas flows• Cleaning cyclone	Once a week
<ul style="list-style-type: none">• Multiple-point sucrose external calibration check using 1, 5, 10 μL of 4.27 $\mu\text{g C } \mu\text{L}^{-1}$ sucrose standard (see Table S2 for results)• Sampling flow calibration with a flow calibrator (tetraCal™, BGI Inc., MA, USA) (Target range = $8.0 \pm 0.4 \text{ L min}^{-1}$ local condition)	Once every month
<ul style="list-style-type: none">• Replace carbon-impregnated filters of the denuder• Perform dynamic blank experiment to check organic vapor removal efficiency. A 47-mm Teflon filter was placed upstream of the denuder to remove particles and the analyzer was set to operate in a 2-h cycle to analyze the amount of organic vapor adsorbed on the quartz filter substrate during 1-h sampling (see Table S2 for results)	Once every 1–2 months

Table S2. Results for quality control work for hourly OC–EC measurement during this study including recovery (%) of sucrose external calibration check, instrument blank, method detection limit and dynamic blank test

Year	Sucrose external calibration recovery			Instrument blank ($\mu\text{g C}$)		Method detection limit ($\mu\text{g C m}^{-3}$)		Dynamic blank OC ($\mu\text{g C m}^{-3}$)
	4.27 $\mu\text{g C}$	21.4 $\mu\text{g C}$	42.7 $\mu\text{g C}$	OC	EC	OC	EC	
2011	N/A*	101.7	100.9	0.20±0.18	0.06±0.10	1.48	0.78	N/A*
2012	105.8	97.5	88.3	0.21±0.15	0.00±0.01	1.23	0.09	0.99±0.18
2013	124.4	102.0	102.9	0.14±0.15	0.00±0.01	1.21	0.06	0.66±0.21
2014	111.0	101.4	92.4	0.13±0.10	0.00±0.00	0.85	0.01	0.95±0.24
2015	116.2	100.2	96.0	0.09±0.10	0.01±0.02	0.78	0.15	0.62±0.14
2016	112.3	98.4	97.1	0.10±0.10	0.01±0.02	0.83	0.14	0.67±0.36
2017	118.8	102.4	97.3	0.02±0.04	0.00±0.00	0.29	0.01	0.72±0.24

Note: N/A indicates that no relevant test was performed.

Table S3. Comparison of VOCs characteristic ratios among fuel-filling process profile derived in this study and gasoline and diesel fuel profiles reported in Tsai et al. (2006)

	Fuel-filling process (This study)	Gasoline fuel (Tsai et al. 2006)	Diesel fuel (Tsai et al., 2006)
Toluene/Benzene	12.4	22.1±12.7	~10*
Toluene/ <i>m</i> -& <i>p</i> -Xylene	1.8	6.3	~1*
Ethylbenzene/ <i>m</i> -& <i>p</i> -Xylene	0.5	~0.5*	~0.25*

Note: The asterisk indicates that the value is approximated from graphic information as no numerical values were provided in the publication.

Table S4. R², slope and intercept of PMF modeled versus measured concentration of the fitting species in the base run

Species	R ²	Slope	Intercept
Ethene	0.32	0.33	1.54
Ethane	0.40	0.36	1.70
Propane	0.93	0.87	0.77
Propene	0.81	0.93	0.02
<i>i</i> -Butane	0.94	0.89	0.44
<i>n</i> -Butane	0.95	0.87	0.98
<i>i</i> -Pentane	0.88	0.84	0.12
<i>n</i> -Pentane	0.84	0.74	0.09
Benzene	0.83	0.80	0.07
Toluene	0.76	0.70	0.32
Ethylbenzene	0.91	0.74	0.04
<i>m</i> -/ <i>p</i> -Xylene	0.90	0.95	0.00
CO	0.73	0.98	-0.02
NO _x	0.75	0.77	22.2
OC	0.64	0.50	2.37
EC	0.90	0.86	0.60

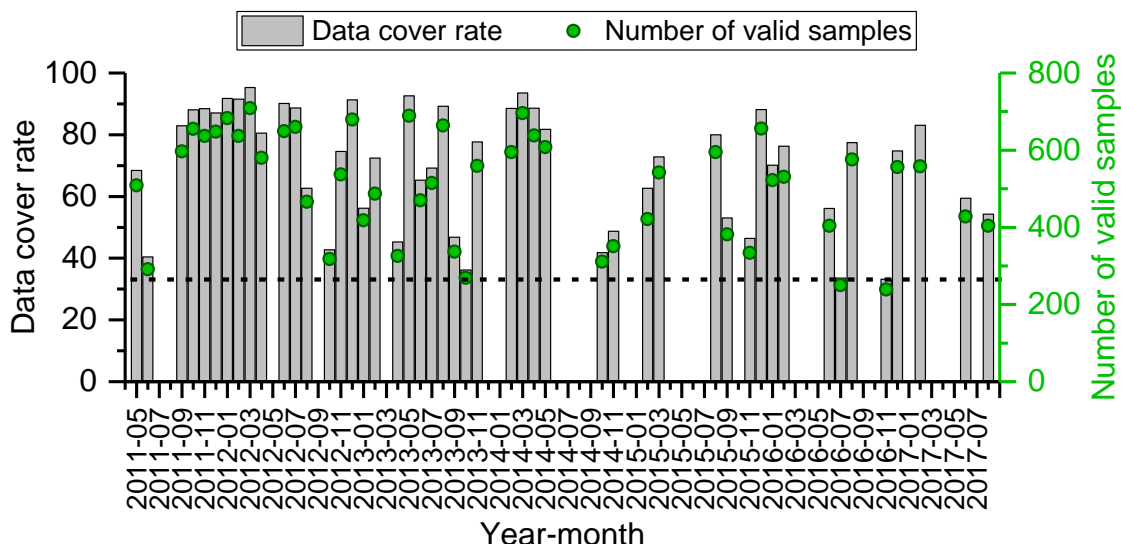


Figure S1. Monthly data cover rates (gray bars, left axis) and numbers of valid samples (green markers, right axis) after excluding hourly samples with one or more missing species and sampling days with a data cover rate < 75%. Data cover rate = Number of valid data divided by the total number of hours during the study period. The dashed horizontal line indicates a data cover rate at 33 %, above which the monthly data were considered in the data analysis of this study.

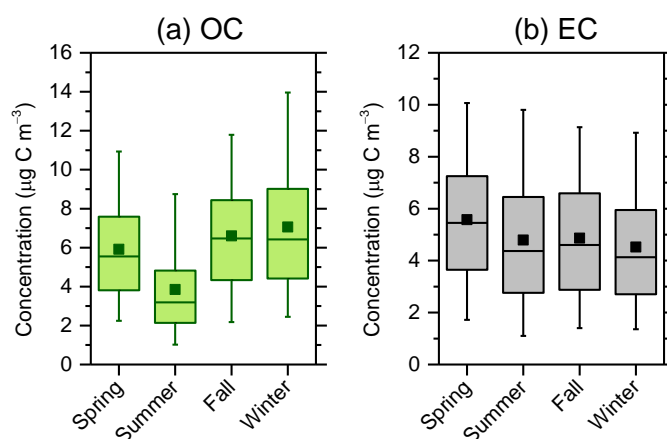


Figure S2. Seasonal variations in (a) OC and (b) EC concentrations at MK AQMS over the entire study period. Square marker and horizontal line within the box represent mean and median, respectively. Lower and upper bounds of the box represent 25th and 75th percentile. Whiskers represent 5th and 95th percentile.

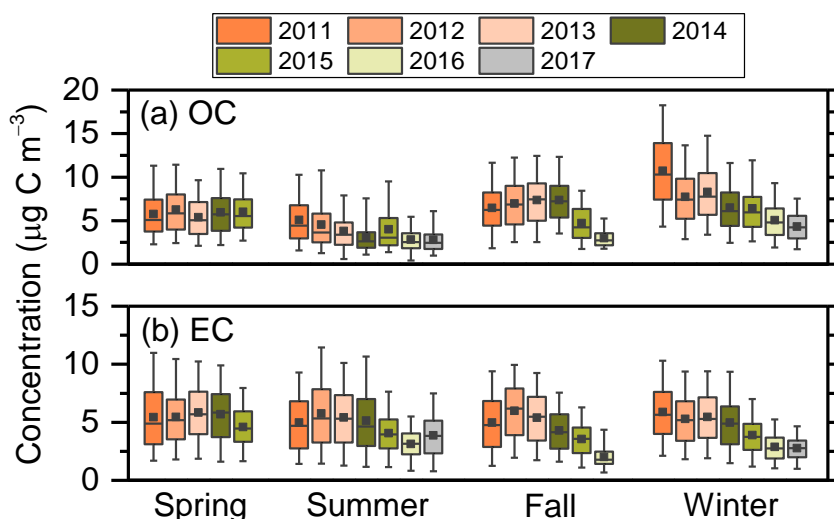


Figure S3. Inter-annual trends of (a) OC and (b) EC at MK AQMS from 2011 to 2017 during spring (mid-March to mid-May), summer (mid-May to mid-September), fall (mid-September to mid-November) and winter (mid-November to mid-March of next year). The measurement did not cover spring 2016 and 2017 and fall 2017, thus their results are not shown. Square marker and horizontal line within the box represent mean and median, respectively. Lower and upper bounds of the box represent 25th and 75th percentile. Whiskers represent 5th and 95th percentile.

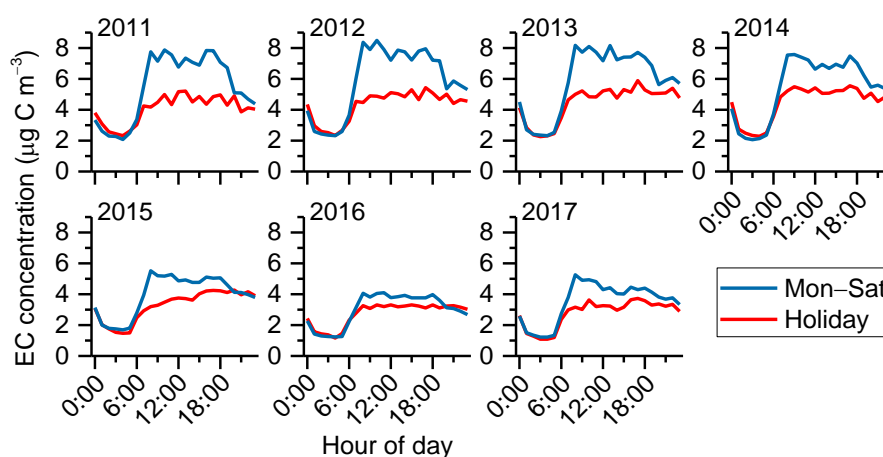


Figure S4. Diurnal variations of EC concentrations at MK AQMS from 2011 to 2017. Monday–Saturday data are indicated by blue lines, Sunday and public holiday data are indicated by red lines.

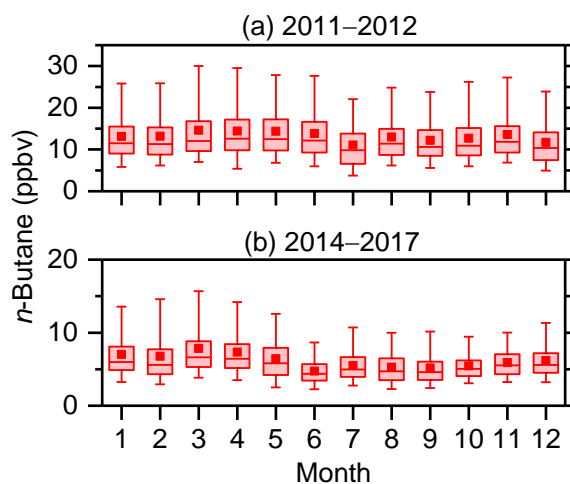


Figure S5. Monthly variation of *n*-butane concentration during (a) 2011–2012 and (b) 2014–2017 at MK AQMS. Data from 2013 is not included because a major catalytic converter replacement program for LPG-fueled vehicles was undergoing and *n*-butane showed a precipitous drop during that year. Square marker and horizontal line within the box represent mean and median, respectively. Lower and upper bounds of the box represent 25th and 75th percentile. Whiskers represent 5th and 95th percentile.

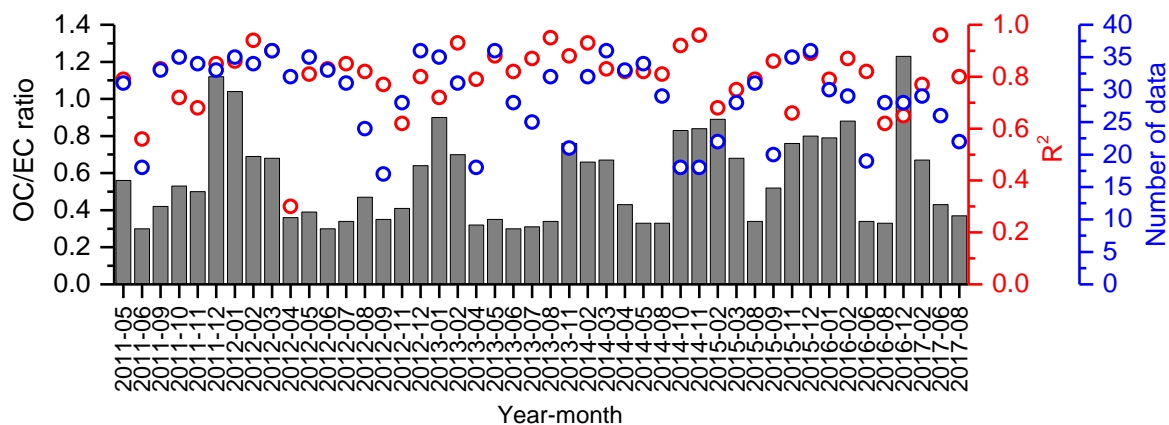


Figure S6. Month-by-month OC/EC ratio (gray columns), R^2 of OC and EC (red markers) and number of data points considered (blue markers) at MK AQMS determined by the optimal Deming regression of the lowest 5 % data by OC/EC ratio for all sampling months. Minimum number of data point considered for each month is 17.

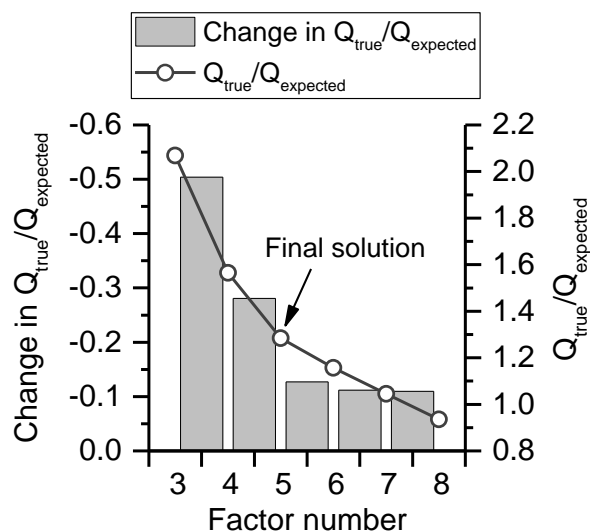


Figure S7. PMF performance in terms of the fitting between modeled and measured species concentrations expressed in $Q_{\text{true}}/Q_{\text{expected}}$ values, considering different factor numbers. Columns show the change in $Q_{\text{true}}/Q_{\text{expected}}$ values as the factor number increases by one (left axis). Markers show the $Q_{\text{true}}/Q_{\text{expected}}$ values in individual runs (right axis). The final solution of the 5-factor run is indicated by an arrow.

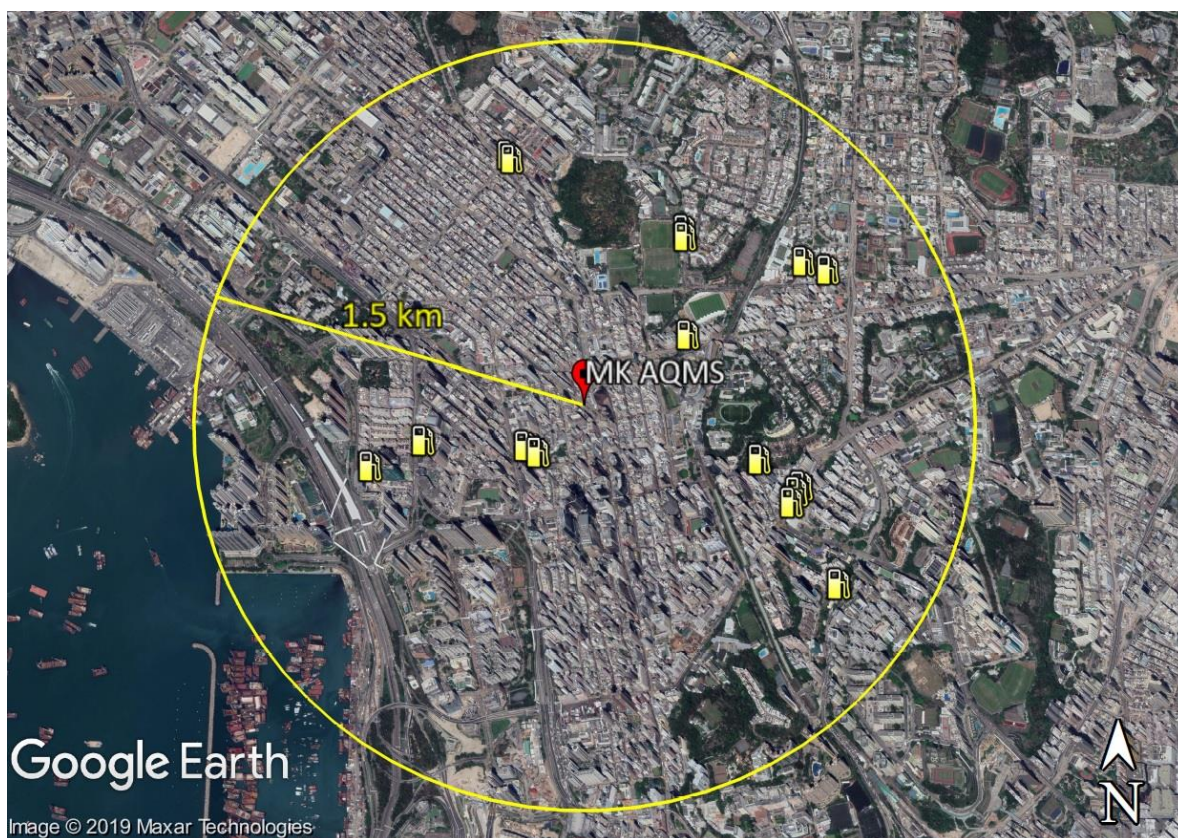


Figure S8. Location map of the gas stations situated within 1.5 km from MK AQMS. The figure was downloaded from Google Earth Pro on 2 January 2020. See following link for the popular times of the gas stations: <https://www.google.com/maps/search/%E6%B2%B9%E7%AB%99/@22.3229513,114.1648924,15.75z>

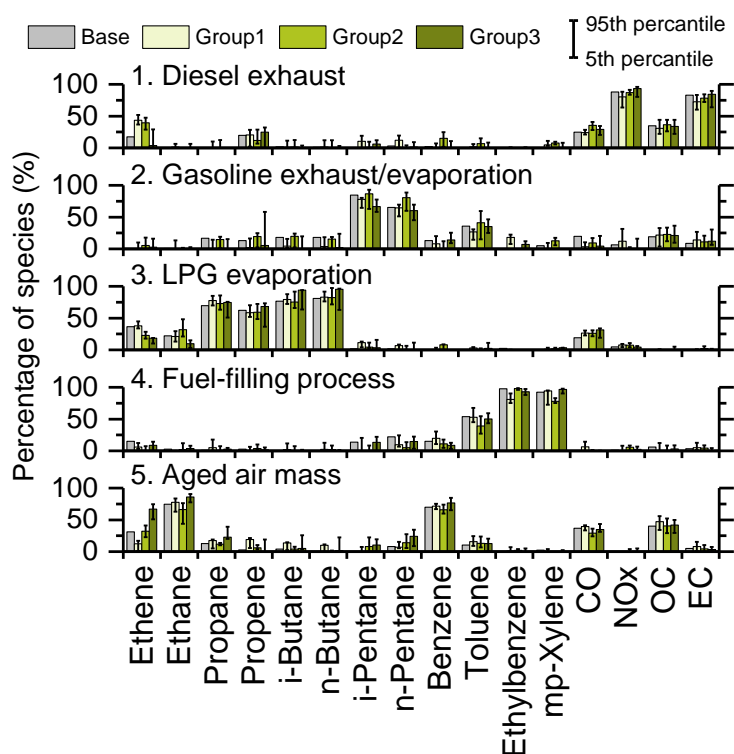


Figure S9. Comparison of factor profiles resolved by PMF modeling with (green bars of different gradients) and without (gray bars) dividing the input samples. The base run considers all 24586 samples spanning from 1 May 2011 to 31 Aug 2017, while group 1, 2 and 3 consider 8191 (1 May 2011–13 Nov 2012), 8185 (14 Nov 2012–21 May 2014) and 8210 (22 May 2014–31 Aug 2017) samples, respectively. Upper and lower bounds of error bars represent the 95th and 5th percentile results, respectively, of the bootstrap analyses.

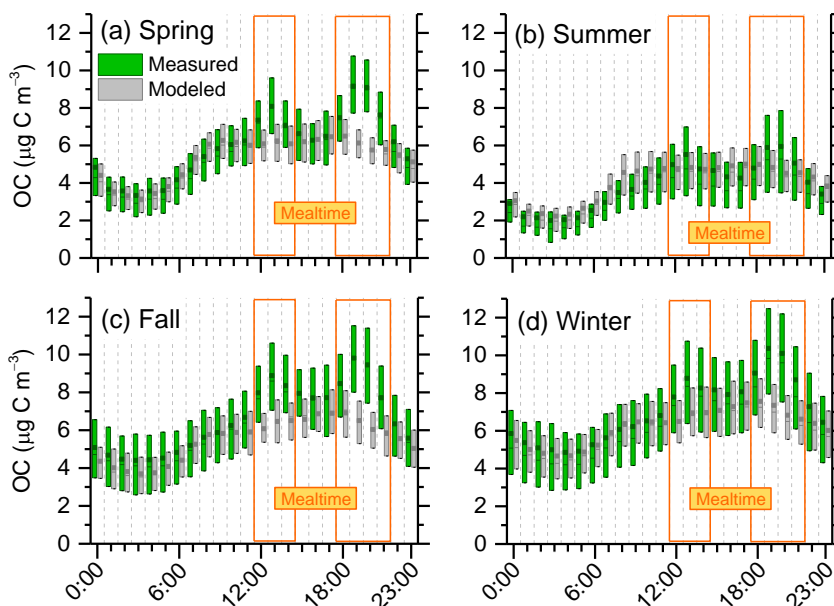


Figure S10. Diurnal variations of OC concentrations in box-plots derived from ambient measurement (green boxes) and PMF modeling (gray boxes) during (a) spring, (b) summer, (c) fall and (d) winter. For each box, solid square marker, horizontal line, lower and upper bounds are mean, median, 25th and 75th percentile, respectively. The afternoon and evening mealtime periods are indicated in the orange frames in each plot.

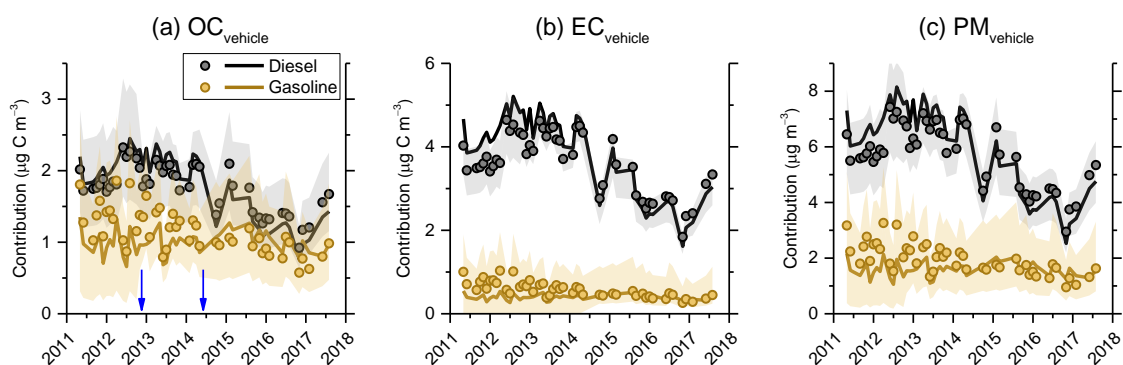


Figure S11. Trends in (a) OC_{vehicle} , (b) EC_{vehicle} and (c) PM_{vehicle} concentrations from diesel (gray markers) and gasoline vehicles (brown markers) at MK AQMS estimated by grouped PMF model, where the input sample data matrix was split into three groups of same sample size for modeling. Blue arrows in the bottom of figure (a) indicate the split points in the grouped PMF modeling. Each marker represents the monthly average of hourly data. Only months with a data cover rate $> 33\%$ are considered. Lower and upper bounds of shaded areas represent the monthly averages of the 5th and 95th intervals, respectively, of the grouped PMF bootstrap results. Solid lines in each plot represent the contributions derived from the base PMF model for comparison with the grouped PMF model.

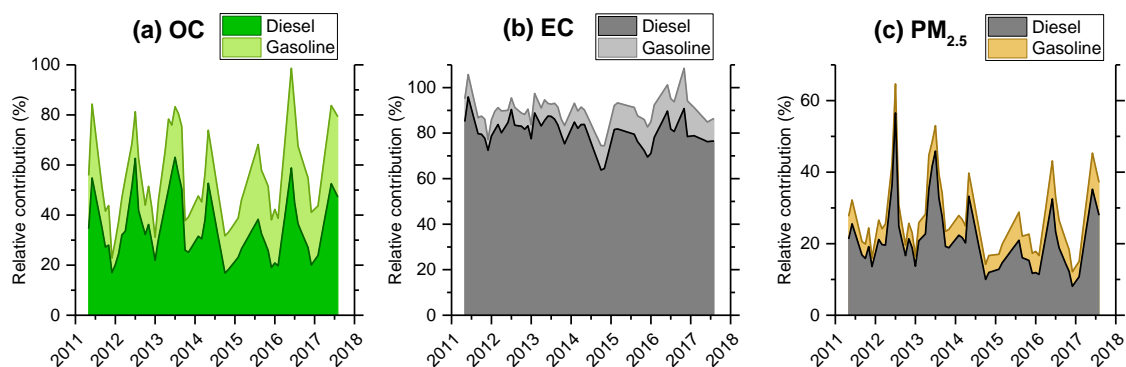


Figure S12. Relative contributions of diesel and gasoline vehicles to (a) OC , (b) EC and (c) $PM_{2.5}$ at MK AQMS. The stacked areas are constructed by interpolation of the monthly data points. Only months with a data availability rate $> 33\%$ are considered.

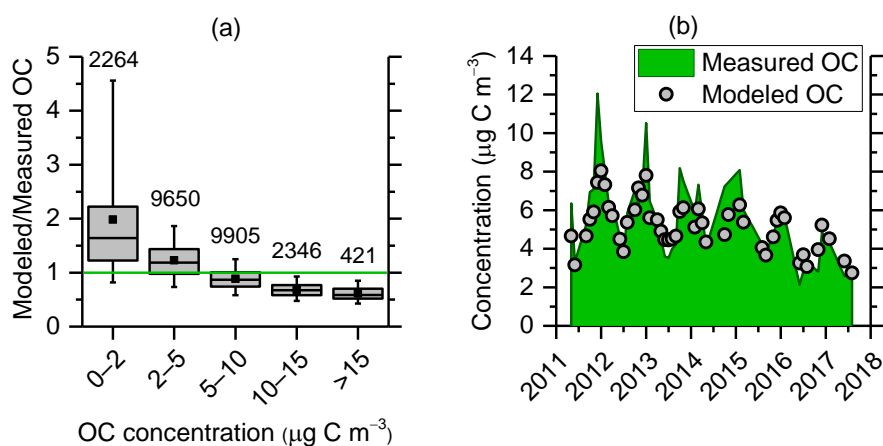


Figure S13. Comparison of PMF-derived and measured OC concentration at MK AQMS. Figure (a) presents the result as modeled-to-measured ratio in box-plot as a function of ambient OC concentration. Square marker and horizontal line within the box represent mean and median, respectively. Lower and upper bounds of the box represent 25th and 75th percentile. Whiskers represent 5th and 95th percentile. The figures above each box diagram represent sample size. Figure (b) presents the comparison over time, with green area and gray markers representing measurement and modeling results, respectively.